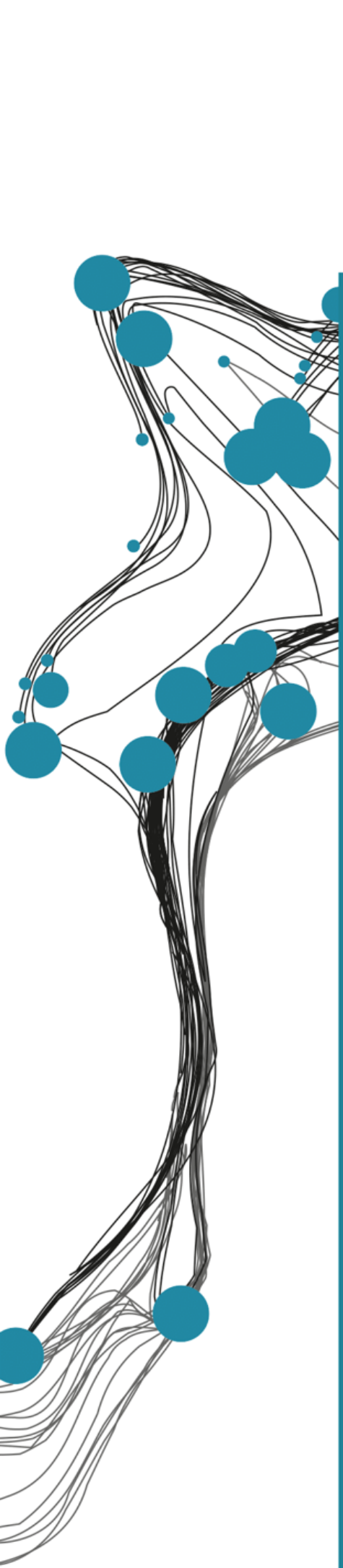

UNIVERSITY OF TWENTE

BACHELOR ASSIGNMENT
FACULTY OF SCIENCE AND TECHNOLOGY
MD & I

The impact of Coiled Embolization on AVM blood flow using Tabletop MR Imaging

8-07-2024

Anouk Bakker s 2728575

Committee

Chair and daily supervisor: Frank Simonis

Member: Wyger Brink

External member: Erik Groot Jebbink

An arteriovenous malformation (AVM) is a vascular anomaly characterized by an abnormal connection between an artery and a vein. This study aims to assess the effects of coiled embolization on blood flow within an AVM. To achieve this, a custom-made coil model was developed and in combination with a 3D-printed AVM model. Blood flow dynamics were examined using 4D flow MRI measurements conducted on a tabletop MRI. The results show that coiled embolization, performed with a handmade coil and catheter in an AVM phantom, disrupted the direct flow through the AVM. This was evidenced by an increased spread of vector lengths in the flow direction and heightened curl within the coil and the aneurysmal zone of the AVM. This circulation is also shown in the flow profile. For future applications, 4D flow MRI could be used to generate additional data for validating computational fluid dynamics (CFD) models. Incorporating a (simplified) capillary network surrounding the AVM would provide insights into the increased resistance of a coiled AVM and its effect on blood flow through the capillaries. Ensuring stationary AVM conditions, with no rotation between measurements, would further enhance the accuracy of these models. This research shows a small step towards creating complete AVM CFD models that could enhance and optimize embolization interventions.

Contents

Chapter 1

Introduction

An arteriovenous malformation (AVM) is a malformation in the vascular system, in which there occurs an abnormal short circuit between an artery and a vein. Normally, the capillary bed acts as a resistance, lowering blood pressure and facilitating the exchange of gases and nutrients. In an AVM, this is bypassed and the inefficient flow of blood to the tissues leads to an inadequate supply of oxygen, nutrients and removal of metabolic waste. In addition, venous structures are exposed to high arterial pressures to which they are not resistant, they become damaged and eventually rupture [2]. AVMs can occur anywhere in the body, but are most common in the brain and neck region (47.4 %) followed by the extremities (28.5 %). [3]

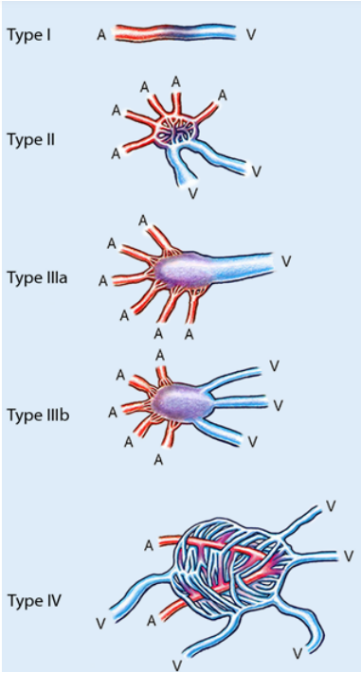

Figure 1.1: The Yakes classification, A artery, V vein [1]

Usually AVMs are already present at birth but are dormant. Superficial AVMs are mostly detected during childhood, because they grow into highly vascularised masses below the surface of the skin. If an AVM is deeper in the tissue, it will progress unnoticed for longer. Hormonal factors are known to trigger the progression of an AVM, such as puberty, pregnancy, or trauma. These cases become problematic in the early adulthood. [3] Complaints per AVM location vary in the brain for example, AVMs can be discovered by investigating an acute intra cerebral haemorrhage. However, they are also often discovered as an incidental finding during investigations for conditions such as chronic headaches and seizures [2]. AVMs are the most complex type of congenital vascular malformation and affect both the arterial and venous systems. The AVMs can be classified by different mechanisms, in this research the classification described by W.Yakes [1] will be used. The Yakes classification is based on the number of feeding arteries and veins, as shown in figure 1.1.

1.1 Treatment possibilities

There are three main ways to treat an AVM. The first is to remove the whole AVM surgically, this is a long and precise operation. Only smaller and superficial AVM are suitable for this. A non-invasive way to treat AVMs is with stereotactic radiotherapy. Radiation beams focused on the AVM cause thickening of the vascular wall, which leads to slowing the blood flow and eventually clotting of the AVM. A treatment like this takes two to four years and is only possible for small AVMs. For this research, treatment with coils (embolisation) will be considered. A catheter is passed through the inguinal artery to the AVM, where the coil is placed on the arterial side of the AVM. This blocks the AVM and promotes the blood to go through the surrounding capillaries. The AVM is not completely eliminated, but the flow through the AVM diminishes. This method is mostly used for larger AVMs located in critical regions of the brain [4]. This research will investigate the flow dynamics in an AVM as a result of coiled embolisation.

1.2 Cardiovascular modelling

Numerical and experimental models of cardiovascular disease have gained significant attention for their applications in haemodynamic studies. These models can also be used to validate imaging techniques and support clinical decision making in complex vascular pathologies. However, due to the challenges of modelling AVMs, the application of these techniques to AVM management is still in its early stages. AVM have a highly complex feeding and draining patterns in combination with serval types of tissues, this makes distinguishing which arterial channel directly drains into the venous system very hard. An essential part of creating these models is the validation of the model against haemodynamic data. This is now done by clinically easy available techniques, such as digital subtraction angiography (DSA) images and Computed Tomography (CT). DSA provides excellent vascular images, angioarchitecture and flow distribution.[5] However, this is associated with high cumulative contrast and radiation doses. Moreover, as was mentioned by *Franzetti et al.*, the main flaw of deriving flow information from CT and DSA is the lack of modalities to quantitatively assess AVM haemodynamics. Even when the feeding arteries van be identified with DSA the complex vascularization and flow patterns are difficult tho predict. Magnetic resonance imaging (MRI) is a non-invasive alternative method for these measurements, specifically 4D flow MRI, which adds the dimension time and makes flow visualisation possible.[5]

In this research, 4D flow MRI measurements will be used to measure the flow effects of coiled embolization in a modelled AVM. The ultimate goal is a complete computational fluid dynamics (CFD) for AVMs that makes patient specific treatment recommendations. This CFD could be used to predict the embolic agent dosage required to achieve a successful embolisation, and inform and optimise the embolisation intervention. [6]. Producing this CFD is beyond the scope of this research. This research focussed on producing validation data for such a model. This leads to the research question, **What are the flow effects of coiled embolisation on the flow in a modelled AVM (type I)?**

1.3 MRI flow

Before the modelling process will be explained, a further clarification of the complex principle of 4D MRI is needed. MRI uses a strong magnetic field and radio waves to image the hydrogen atoms in the body, resulting in detailed images of the structures in the body. The temporal expect, making it 4D, is added by velocity-encoded phase contrast MRI.

Phase contrast MRI uses bipolar gradients to distinguish moving and stationary particles. A bipolar phase encoding gradient is applied in a pair of a positive and negative pulse, both of the same magnitude and duration. A stationary spin will experience no net phase shift because the effect of the positive and negative pulses cancel each other out. A moving spin on the other hand will experience a net phase shift which is proportional to its velocity. Therefore, not only can the stationary and moving spins be distinguished, but the velocity of the moving spins can also be calculated. The bipolar gradient applied in the x-axis provides the flow in the x-direction respectively, for y and z. [7]
The amplitude, duration, and spacing of the bipolar gradients determine the degree of sensitivity to slow or fast flow. VENC, short for Velocity Encoding, is the parameter that determines this. The VENC must be specified prior to a measurement and should be the highest velocity in the imaged region in m/s. The VENC value can be measured in the positive and negative direction, this is encoded by the phase shifts spanning from - 180° to +180°. If the actual velocity is higher than the select VENC, the phase shift will surpass 180° and can no longer be distinguished from a phase shift in the negative direction. So the flow that is too high will be truncated and projected as a negative flow. This is known as aliasing. The VENC can also be set too high, this adds extra noise and makes it difficult to detect small flow differences. [8]
A conventional MRI, as is used in hospitals is a slight overkill for the model, which is only 7.5 cm long. Therefore, a table-top MRI (Magspec, Pure Devices GmbH, Rimpar, Germany) is used. The principles of both MRIs are the same but on different scale. In addition, a conventional MRI is very expensive compared to a table-top MRI.

Chapter 2

Methodology

In order to study the effects of coil embolization on AVMs, it is essential to first create an accurate model of the AVM, the coil and the blood. In this research, we utilized velocity encoded MRI measurements to collect the flow data. This allows for measuring and analysing the flow dynamics within the AVM and the effect of coiling.

2.1 AVM modelling

The model for the AVM was already provided by previous research by J. Bougardt. This specific AVM was modelled based on a AVM in the lower leg [9]. The feeding artery of this AVM is the posterior tibial artery, this artery supplies various muscles of the posterior compartment (often referred to as the calf) and the tibia bone of blood. [10] The 3D model, as is shown in figure 2.1, was derived from a CT-scan. To ensure a waterproof model, a resin printer was used. The model was printed with clear resin, which makes it easier to check for air bubbles before measuring.

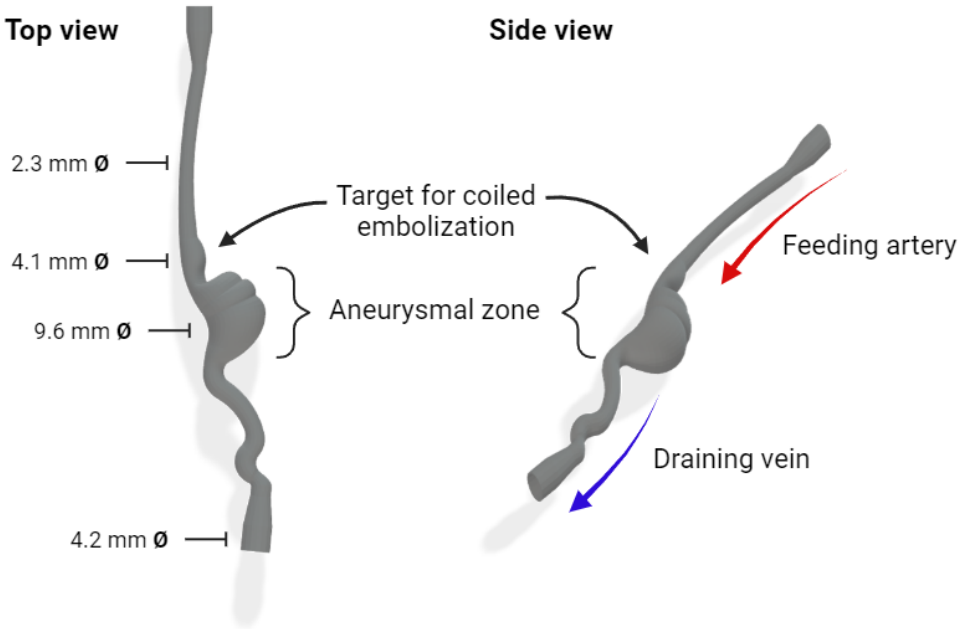

Figure 2.1: The modelled type I AVM used for this experiment, Left: top view, Right: side view with the feeding artery and draining vein.

The bore of the used table-top MRI is $15mm$ and the width of the AVM was originally greater than $15mm$. Therefore, the model is scaled to fit into the MRI with a factor of $2/3$. The scaled dimensions are shown in figure 2.1. The diameter of the tube which the fluid moves through effects the flow, so when the diameter is scaled the inlet flow needs to be adjusted to this. This is done by matching the Reynolds numbers of the scaled and unscaled version. The scaling results in a factor of $2/3$ in the velocity. The coil model is in ratio with the AVM, so the size of the coil is also effected. This has to be taken into account with producing the coil.

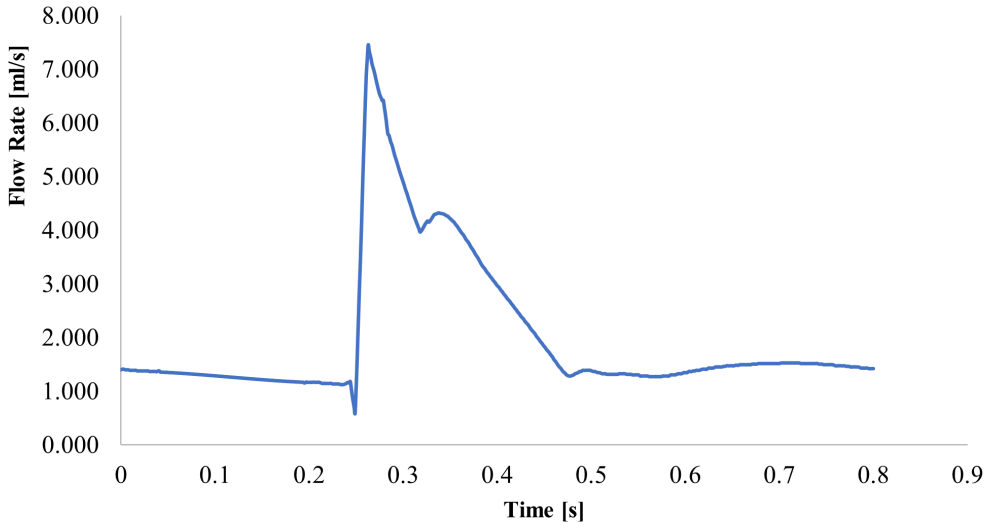

Figure 2.2: The flow rate (ml/s) in the AVM plotted against the time (s)

2.2 Flow velocity

The blood pressure supplied by the artery is time-dependent, so the flow rate varies between $0.500ml/s$ and $7.400ml/s$. The pulsatile flow profile is shown in figure 2.2. The mean flow of this pulse is $2ml/s$. The pulse data is provided in combination with the AVM model by J. Bougardt. It has to be taken into account that this data is not yet scaled to the factor $2/3$ as described before, this will be done by calculating the VENC values. These VENC values are dependent on the maximal speed in the AVM. Mimicking the pulsatile flow was not in reach for this research. Thus, the flow velocity is kept constant during a measurement and only the mean value is measured.

2.3 Blood mimicking fluid

Blood appears to be a homogeneous liquid, but microscopically it is a suspension of the formed elements in a fluid matrix, the plasma. Because of these formed elements, blood has a higher density and viscosity than water. [11] However, blood's viscosity is not constant. At higher shear rates, the viscosity reduces, which makes whole blood non-Newtonian and shear-thinning fluid. [12] For this study, only the formed elements will not be modelled, a fluid is made that replicates the shear-thinning properties of whole blood. The so-called Blood Mimicking Fluid or BMF. The BMF is a mixture of distilled water ($95wt\%$), glycerol ($4.93wt\%$), and xanthan gum ($0.07wt\%$). This combination is inspired by *N. Perrira et al*, as was published in Journal of Physics.[13]. Previous rheological experiments by J. Bougardt led to this combination, these results and preparation methods are show in Appendix A.

2.4 Coiled embolization

With the AVM type presented here, a coiled embolization would be preformed with MReye® Embolization Coil, which is a $0.89mm$ (0.035 inches) wire diameter platinum coil. There are multiple coiled diameters and coil lengths available, for example the coil shown in figure 2.3. With this AVM the coil would be placed with the coaxial technique, this means that coils are placed behind each other until the vessel is blocked [14]. However, in this simplified model, only one coil will be placed. This coil will keep its coiled shape and is therefore easy to replicate in a CFD model. Just placing a conventional platinum coil is not possible for different reasons. These complications are transcribed to three requirements.

Figure 2.3: Photo of MReye Embolization coil, with its dimensions

First of all the coil cannot be made of a metal. As is mentioned in the safety sheet of the coil, the coil is MR safe but causes artefacts. The image artifact extends approximately 12*mm* from the coil with a gradient echo pulse sequence and a 3.0 Tesla MRI system [15]. The risk of artefacts needs to be avoided because it would influence the flow measurements too much.
Secondly, the coil must be placed in the AVM model and kept in the same position throughout the measurement. In vitro, the coil is delivered with a catheter. The correct place of the coil is determined with a guide wire, the catheter is placed over the guide wire to the target location. The guide wire is then removed while the catheter says in the same place. Then the inner catheter with the coil delivery mechanism is pushed through the catheter until it reaches the target location. Finally, the coil is left behind, and the catheters are removed. [14]
And lastly, the AVM is resized to $2/3$ of its original size. Therefore, the coil also needs to be resized. In the designing of the catheter mechanism, this has to be taken into account as well.

2.4.1 Developing the coil

Before the coil can be designed, the dimensions need to be specified. The wire diameter in a real coil is 0.9*mm*, thus the scaled version must be 0.6*mm*. The outer diameter of the targeted location of the coil is measured at 4.1*mm* and the resin printed walls are 0.4*mm* thick, which makes the inner diameter 3.3*mm*. In vivo coils need to be oversized by about 25% [16] however this is a plastic model. Therefore, it is assumed that this would not be necessary. The coil should be big enough to stay in place while the BMF flows through. Experimental testing showed this goal was reached by a coil with a coiled diameter of 3.4*mm*. The length of the coil is determined by the amount of loops, which depends on the AVM and application technique. In this case, four loops were chosen to keep the applied resistance simple and easy to model.

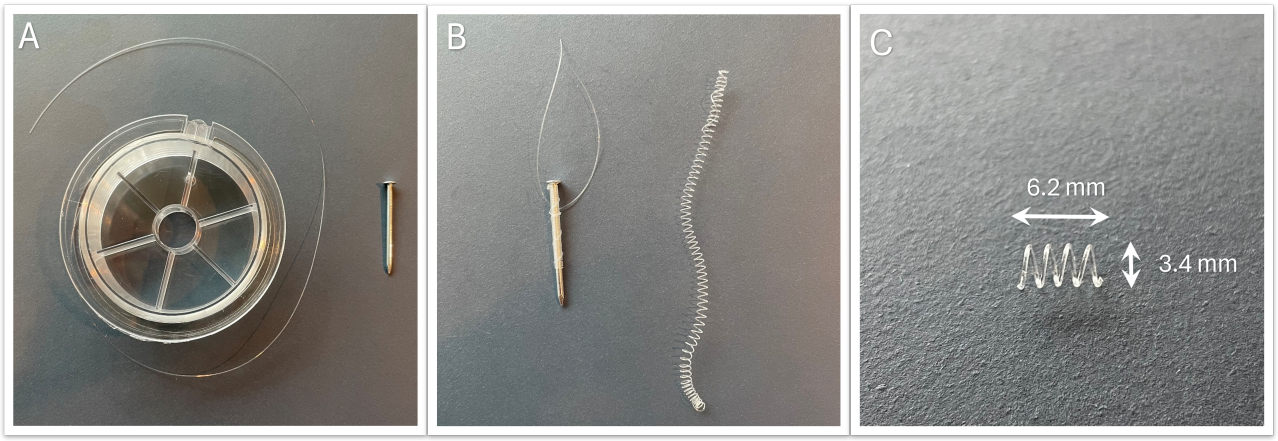

Figure 2.4: The production of the coil shown in sub figure A B and C

The coil is made from nylon wire from a construction market. Nylon is a strong but flexible material and does not absorb water [17]. The melting temperature of nylon varies by grade, but lays around 200 °C) [18]. When nylon is heated below its melting point, it holds the solid form but becomes formable and holds its new form when cooled down. This property is used by producing the coils. For the wire to take on its coiled shape, a nail was used with a diameter of 2.2*mm* (figure 2.4 A). The wire was wrapped around the nail very tightly, as is shown in figure 2.4 B. These were then warmed up to 100°C in a boiling pan for 3 minutes. When the nail was completely cooled down, the wire was taken and the coil is revealed. The coil is then cut to the right size. In this case, 4 loops long.
However, when a 0.5*mm* plastic wire is used, a with 0.035 inch catheter. The catheter does not fit into the modelled AVM. When searching for a smaller catheter option, Pediatric Arrowg+ard Blue® Two-Lumen CVC was found. This does fit inside the AVM and makes located delivery possible. The plastic coil form 0.5*mm* does not fit inside of this. However, a 0.3*mm* coil does fit inside. Therefore, the choice was made to use a smaller coil, the production procedure stayed the same.

2.4.2 Catheter

A was mentioned earlier, a normal 0.035*inch* catheter was not possible for this model because the feeding artery was too small. Therefore, the Lumen CVC was used. To prepare the Two-Lumen catheter, it was cut as is shown in figure 2.5A. The part as is shown in figure 2.5B is 8*cm* long and has a diameter of 1.40*mm*. The 0.3*mm* coil was pushed inside the catheter, at the blue tip. In figure 2.5 B the white arrow points at the coil halfway into the catheter. In sub figure 2.5 C the coil is pressed in completely and the other side of the catheter is loaded with a 0.5*mm* nylon wire. This has a larger diameter than the coil, but still fits into the catheter and therefore pushes the coil out. In this way, the delivery of the coil can be done location specific.

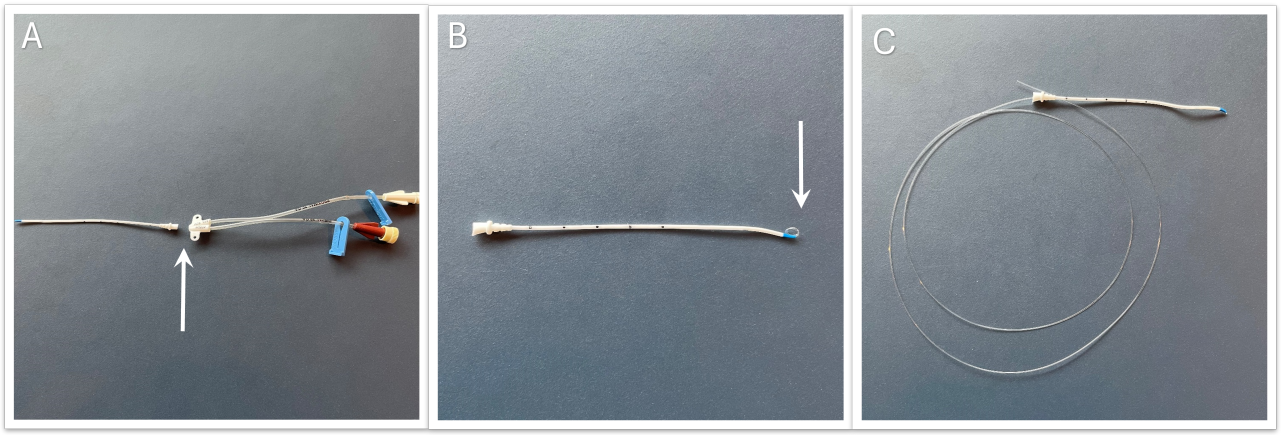

Figure 2.5: The production of the coil shown in sub figure A B and C

2.4.3 Implementation of the coil

The short catheter limits the possibilities to deliver the coil while the BMF is flowing through the AVM, therefore the coil is placed in the empty AVM. Figure 2.6 shows the process of the implantation of the coil. First, the catheter is moved through the supplying artery to the target of the coiled embolization. When this is reached 2.6 B, the 0.5*mm* wire is pushed slowly further into the catheter. The coil can be seen, slowly coming out of the catheter and coiling in to its original form. When the whole coil is pushed, the catheter including the 0.5*mm* diameter wire can be retracted. The coil can be seen in at the target location in figure 2.6 C by the arrow.

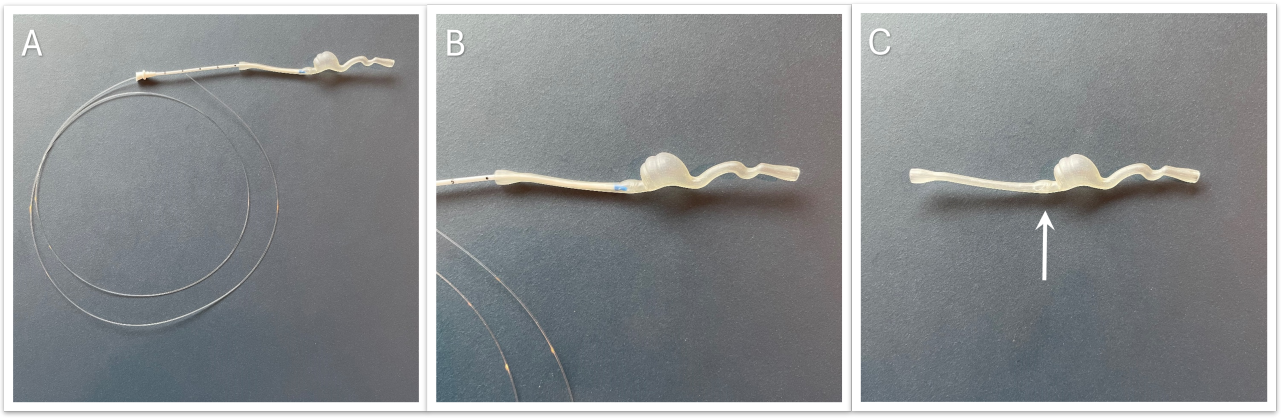

Figure 2.6: The implementation of the coil shown in sub figure A B and C

2.5 Experimental setup

The experimental setup for measuring the flow is shown in 2.1. A table-top MRI (Magspec, Pure Devices GmbH, Rimpar, Germany) is slightly adjusted to an increased bore size from 10*mm* to 15*mm*. This results in an adjustment in the static B0 field from 0.55T to 0.503T. The table-top MRI is warmed up to 37 °C and placed on its side so the tubing with the modelled AVM can fit through. The pump (12V, 0.5*Bar* COMET ELEGANT)

Table 2.2: The mean for the flow (ml/s), scaled flow (ml/s), velocity (m/s) and VENC (m/s)

Flow (ml/s)	Scaled flow (ml/s)	Velocity m/s	VENC m/s
2.000	1.3333	0.3333	0.5

is placed in the BMF and is attached to the supplying (artery) tube. The power supply for the pump is regulated by a Delta electronics power supply (E 0301-1). It is important that the parameters are set, and the air bubbles are all taken out before starting with a measurement. The flow can be adjusted with the clamp and the voltage of the power supply, this is measured with a graduated cylinder and a stop watch.

Table 2.1: A simplified drawing of the experimental set-up

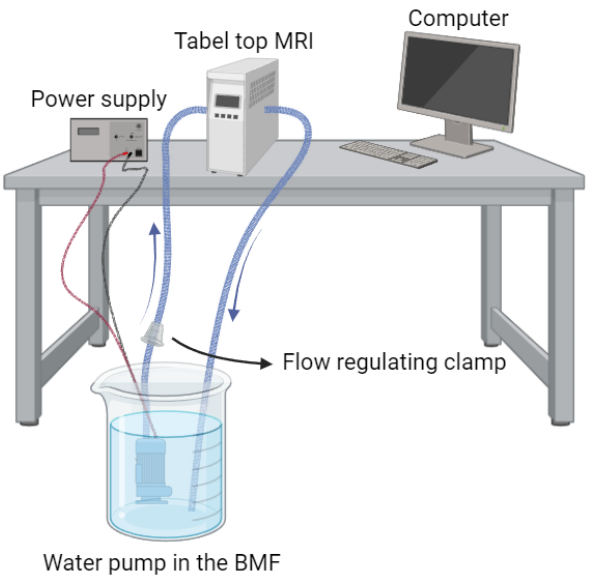

2.6 Table-top MRI

The velocity-encoded phase contrast MRI sequences were provided by Pure Devices© in MatLab code. The data was acquired in a Field of view of 0.020 m x 0.020 m x 0.020 m with the corresponding amount of pixels 148 X 256 x 148. The resolution is set to 0.25 mm for all measurements, and they take around 40 minutes. The VENC values chosen per measurement are essential to avoid aliasing while still being able to detect small differences. The inlet flow shown in table 2.2 are scaled with the factor $2/3$ which leads to the scaled flow for the modelled AVM. The velocity is then calculated for a cross-section of $4mm^2$. Then lastly for the calculation of the VENC a factor of 1.5 is used to estimate the maximal velocity. The Matlab code gives a Velocity3D matrix as output with in the fourth dimension defined as follows: 1 gives the x gradient, 2 the y, 3 the z and 0 no gradient. Measurements were done with a Larmor frequency of 21.43 MHz a T1 value of 0.40 seconds, T2 value 0.20 seconds of and an echo time of 0.0080 seconds.

2.7 Data analysis

All 4D flow data has been pre-processed to correct for eddy currents, this was provided in the Pure Devices© in MatLab code. However, there is still an artefact with in the data that need to be removed before visualisation. This will be done by filtering the RoI. Note that in all analyses, x and y have been swapped, due to an error in the code. After filtering, the data is visualized and quantified.

2.7.1 RoI filtering

The RoI, Region of interest, does not contain any flow information, just the location of the imaged object. When the RoI of the raw flow data is plotted, artefacts are visible on both sides of the AVM, as can be seen

in figure 2.7. This can be removed quite easily by limiting the x and y values of the RoI. The RoI consists of 256x128x128 pixels. For the non-coiled mean flow measurement, the RoI pixels in the x direction were limited to $23 < x > 95$. For the coiled measurement, x and y were limited to $32 < x > 102$ and $35 < z > 96$. These limits are determined by plotting the RoI as a volume against the pixels in the x, y and z direction. Figure 2.7 shows the raw and filtered RoI and exclusion of the artefacts. The filtered RoI will be used in further research.

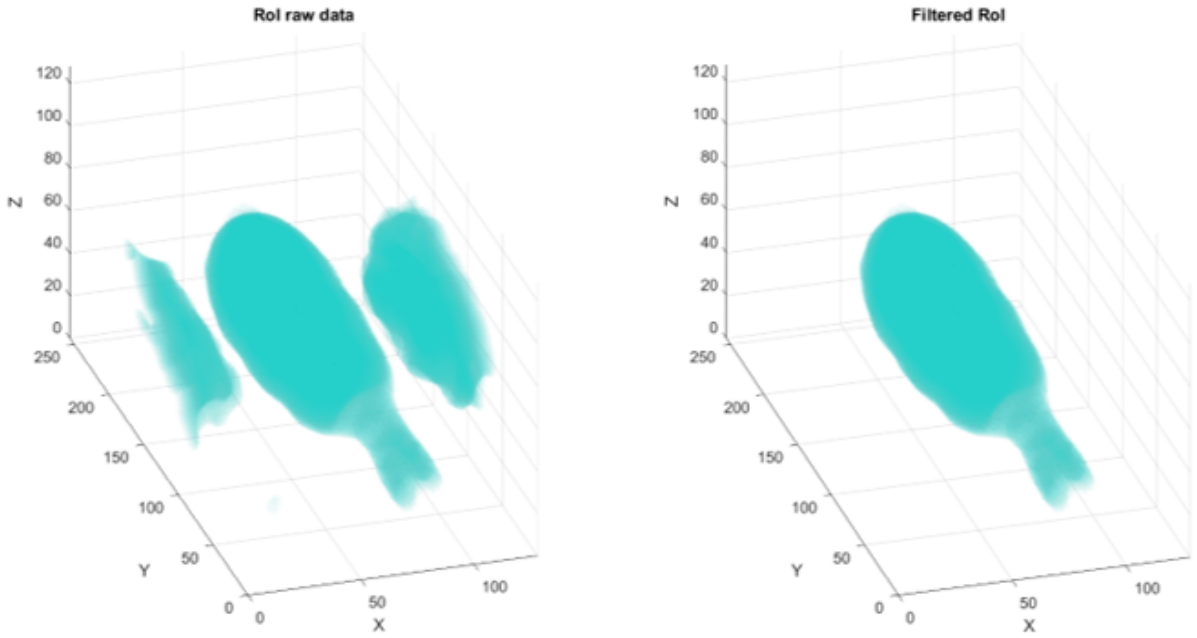

Figure 2.7: The RoI plotted against the pixels in the x, y and z direction, left-hand side: the raw data with on both sides of the AVM artefacts, right-hand side: the filtered RoI by limiting the x values to 23 < x > 95.

2.7.2 Visualisation

The data collected is a 3D volume with a vector in the x, y and z directions at each point in the AVM. The 6D data can be visualised in many different ways, in this research the flow patterns are shown in vector filed and in absolute flow images. Prior to this, the location of the coil is determined with conventional MRI without any flow, a stencil is made to determine the exact location of the coil in the AVM. This will later be used as a template to relate the patterns to the coil location. The flow is first analysed in vector form, showing the absolute flow and the deconstructed flow in the x y and z directions are visualised. These vectors are displayed throughout the volume, with the colour of the vector corresponding to the magnitude of the velocity. The actual flow pattern at different heights is difficult to visualise with vectors alone, so the AVM also displays the absolute flow in slices. By combining such a slice with the coil template, it is possible to see exactly where the coil is located and how this changes the pattern in the flow.

2.7.3 Quantification

To quantify the flow magnitude in the coiled and uncoiled AVM, the x y and z vector lengths are analysed separately. All the length-dataset were not normally distributed, so the median is the best measure for a central tendency. The mean, which is often used, is largely affected by outliers and is robust enough for these data [19]. For the measure of spread, the most robust measure is calculated, the interquartile range (IQR) together with the first quartile and the third quartile. These measures were taken and visualised using a box plot. The outliers are not included with this visualisation.
The curl vector is used to quantify the amount of circulation, this measures the circulation density at each point of the field. The length of the curl vector measures the rate of rotation and is defined as positive for counter-clockwise rotation and negative for clockwise rotation.[20] The absolute length of each curl vector is determined these values are averaged per slice, resulting in an average curl value for each y-pixel. This is

graphed, and shows the magnitude of the circulation density of each pixel along the flow direction (the y-axis). This is done for both the coiled and uncoiled AVM.
Finally, the flow profile is quantified. This is done by taking a cross-section of the supplying artery just before it enters the aneurysmal zone, to make comparison between the AVMs possible. The flow velocity in the y-direction is plotted in 3D with the according values in a colour bar. The final results are presented as a 2D colour map of the velocities. The side view of the 3D plot is also displayed for further examination of the coiled profile. This shows the actual values on the axis, not just on the colour map.

Chapter 3

Results

There are many different ways of presenting the 3-dimensional flow velocities in the x y and z direction. As selection was made to portray the effect of coiled embolization. This includes the vector fields and absolute flow images. The results will be quantified for the vector magnitude, circulation and flow profile. Besides the flow, the coil its self is imaged as well, which will be discussed first.

3.1 Placement coil

Using an available Pure Devices extension, the coiled AVM was imaged from the side. These images were post-processed by increasing the brightness by +20% and contrast by +40%. The coil is indicated by the white arrow in figure 3.1 and digitally zoomed in the corner of this figure. The location of the coil is copied using the red coil that is drawn on in figure 3.2. A semitransparent template is created to visualise the exact position of the coil in figure 3.2, and to determine this location in further analysis.

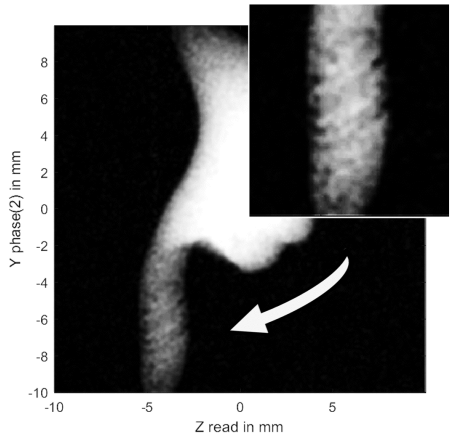

Figure 3.1: The coil location indicated with a white arrow in an MRI image, a further digital zoom in the top right corner.

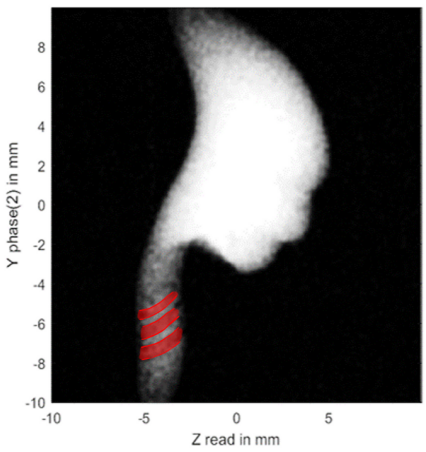

Figure 3.2: The coil location is traced in red.

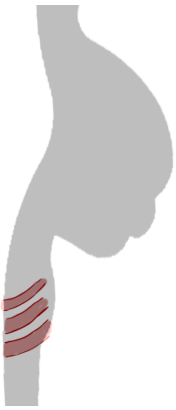

Figure 3.3: The red coil shown in the template.

3.2 Visualisation flow vectors fields

One of the ways to visualize the magnitude and direction of the flow is with vectors. This is firstly done for the absolute flow, followed by the flow of the x y and z direction separately. All vector fields are shown side by side, on the right the uncoiled AVM and on the left the coiled AVM. The vectors in each plot are equally scaled.

3.2.1 Absolute flow vectors

When comparing the vector field shown in figure 3.4 a disrupted flow is seen in the coiled AVM compared to the uncoiled AVM. The flow direction of the fluid through the AVM is along the y-axis, from negative to positive.

The orientation of the AVM and flow direction are shown in the corner of each figure, these stay the same for the upcoming vector fields. The uncoiled vector field shows a stream mostly straight through the AVM, with a slightly heightened flow velocity before and after the aneurysmal zone. The coiled vector field shows more random orientated vectors. It has to be noted that vectors on the surface of the AVM with a large magnitude could also be artefacts. Most of the vectors also point along the y-direction. The stream through the aneurysmal zone is broader than in the uncoiled vector field.

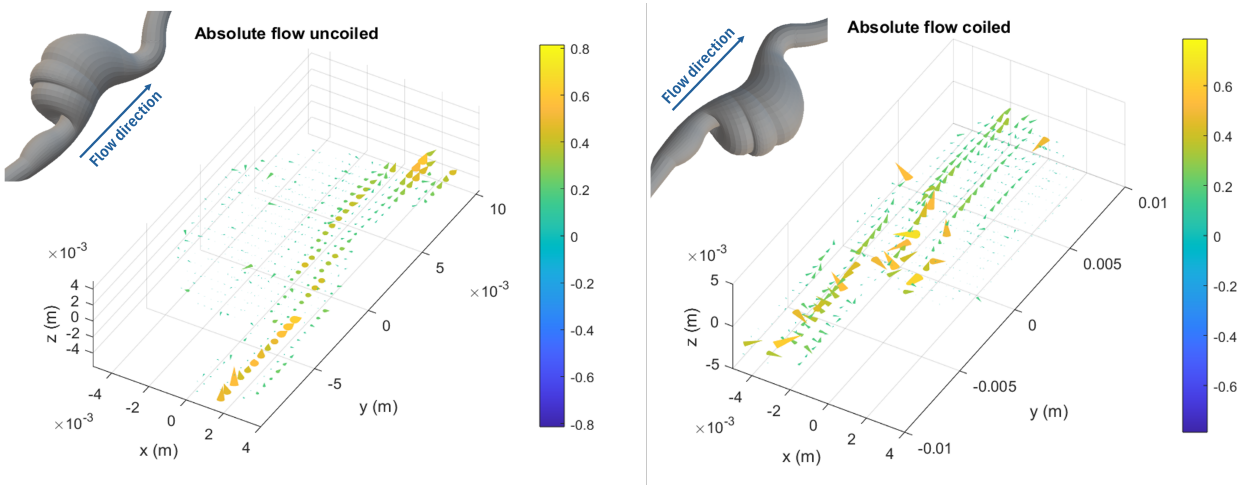

Figure 3.4: The absolute flow vectors displayed with the AVM that is shown in gray. Left: uncoiled, Right: coiled

3.2.2 Vector field in x direction

The subtracted x-flow shows differences between the coiled and uncoiled AVM. The coiled AVM contains larger vectors than the uncoiled AVM. These are mostly in the region of the coil target, and are directed in positive and negative x-direction.

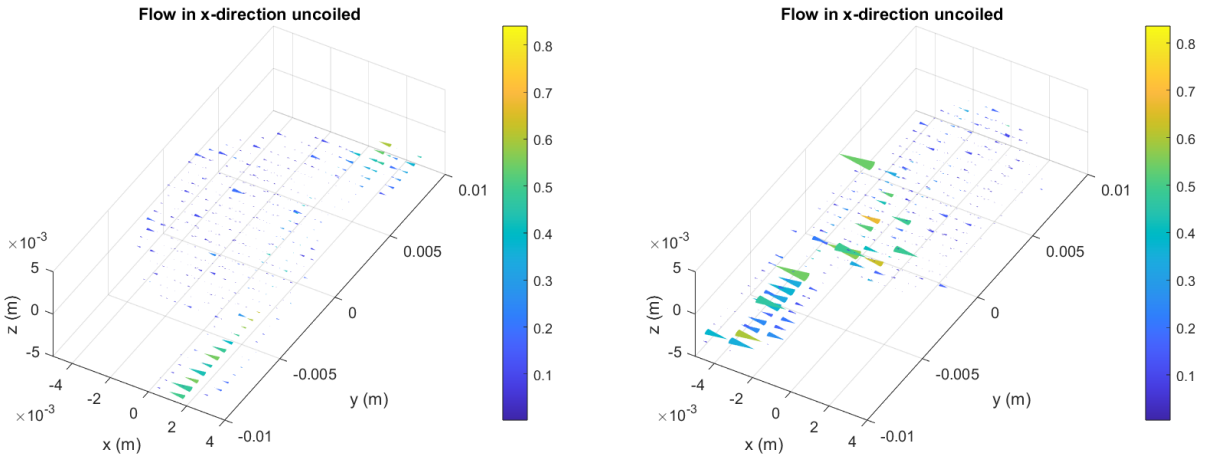

Figure 3.5: The flow vectors in the x direction, Left: uncoiled, Right: coiled

3.2.3 Vector field in y direction

A straight flow through the AVM is clearly visible in both vector filed. However, in the coiled AVM the stream is broader. The coiled AVM shows larger vectors in the aneurysmal zone than the uncoiled AVM. In the whole coiled AVM there are vectors in the opposite direction of the BMF flow, but in the uncoiled AVM negative flow vectors are only viable in the aneurysmal zone.

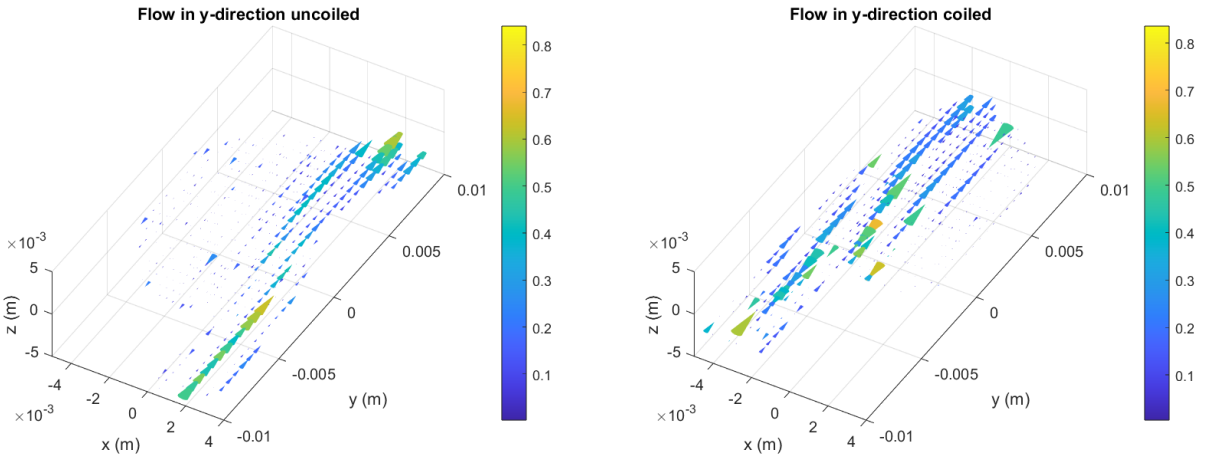

Figure 3.6: The flow vectors in the y direction, Left: uncoiled, Right: coiled

3.2.4 Vector field in z direction

The vector fields in the z-direction are very different. In the uncoiled AVM the path of the straight though flowing BMF shows the largest vectors, these are mostly negative. The coiled AVM has smaller vectors throughout, except for a few larger ones in the aneurysmal zone.

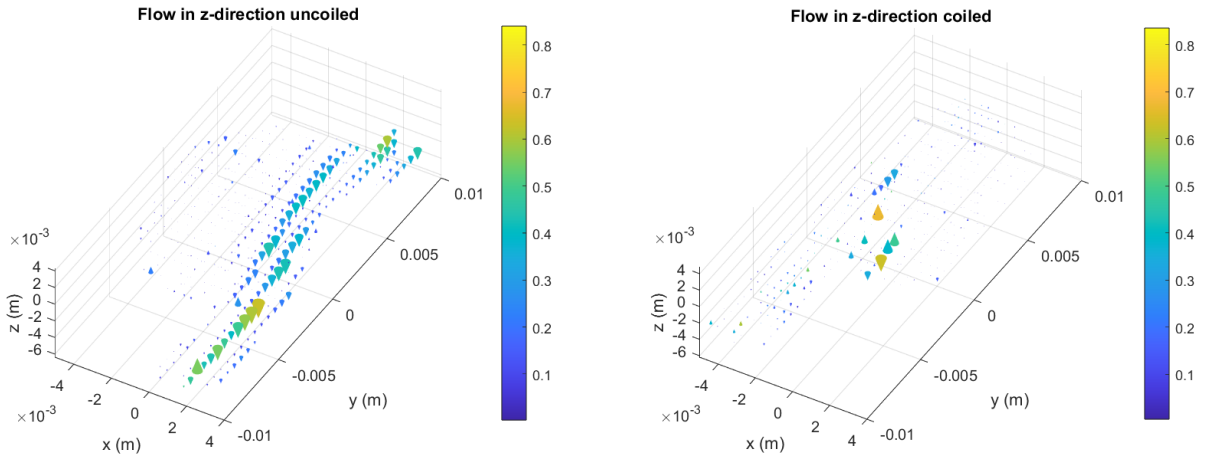

Figure 3.7: The flow vectors in the z direction, Left: uncoiled, Right: coiled

3.3 Visualisation absolute flow

The fluid is pushed though the AVM therefore the highest velocities are expected in the y-direction. Which calculating the absolute velocities, it is assumed that this velocity mostly portraits the flow through the AVM and thus the flow in the flow direction (the y direction). Figure 3.8 shows 12 slices of the absolute flow, these are taken from $z = 40$ until $z = 62$ in steps of 2. The absolute flow velocity (m/s), dimensions of the slice, flow direction and the orientation of the slices are shown in the legend. In the uncoiled AVM a high absolute flow is seen quite straight through the AVM and in the bulge of the aneurysmal zone the flows are close to zero. The highest absolute flow is located at the end of the AVM, where the vessel diameter decreases. The coiled AVM shows a comparable pattern, but not exactly the same. The flow straight through the AVM is less obvious. The highest flows are seen here at the wall in the aneurysmal zone and just before entering the AVM. In the aneurysmal zone, the flow is still close to zero. Finally, the flow before entering the AVM is disturbed and disordered compared to the uncoiled measurement. This is the location of the coil and will be further discussed. The values outside the AVM are shown at a velocity of zero, but actually do not have a value because they are outside the defined RoI.

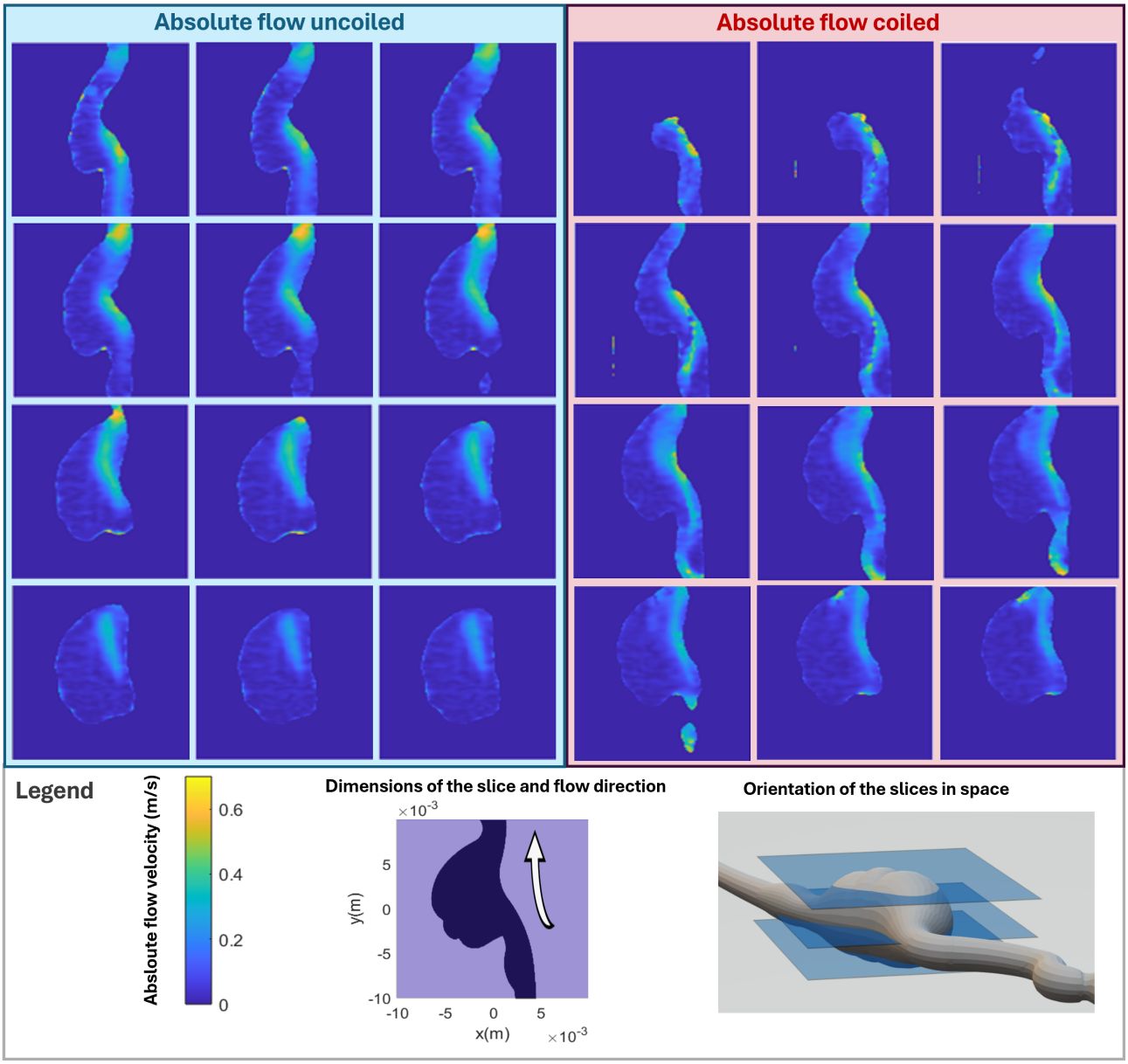

Figure 3.8: The absolute flow in a AVM on the left uncoiled (blue), and on the right coiled (red), displayed in 12 slices (z=40 till z=62). The legend shows the absolute flow velocity (m/s), dimensions of the slice, flow direction and the orientation of the slices

Figure 3.9 shows the location of the placed coil in one of the slices of figure 3.8. The template as is described before is used to determine the exact location of the coil. This shows that the absolute flow before the coil is heightened and when the fluid moves through the coil the velocity decreases. The absolute flow velocity on the right side of the coil is close to zero. Therefore, it seems like the fluid moves through the coil more on the right side. The flow velocity scale is the same as given in the legend of figure 3.8.

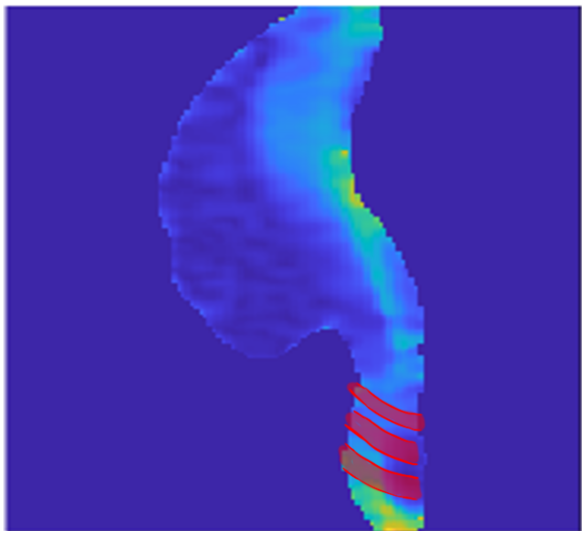

Figure 3.9: Absolute flow with coil drawn in red

Table 3.1: The median, first quartile (Q1), third quartile (Q3) and the interquartile range (IQR) of the length of flow velocity vectors in the x, y and z direction for the uncoiled and coiled AVM.

	Uncoiled			Coiled		
	x	y	z	x	y	z
Median	0.0048	0.0113	-0.0122	0.0004	0.0107	-0.0028
Q1	-0.0128	-0.0026	-0.0486	-0.0178	-0.0062	-0.0148
Q3	0.0205	0.0427	0.0026	0.0185	0.0575	0.0085
IQR	0.0332	0.0452	0.0512	0.0363	0.0637	0.0233

3.4 Quantification

The visualisations shows the patterns of the flow nicely, however this hard to measure. So a quantification is needed.

3.4.1 Quantification vector magnitude

To quantitate the lengths of the vectors in the separate direction the median, first quartile (Q1), third quartile (Q3) and the interquartile range (IQR) are calculated and shown in table 3.1. This is used to make the box plot in figure 3.10. The red boxes show the coiled measurement and the blue boxes the uncoiled measurement. In this box plot the outliers are not drawn, outliers are defined as a value that is more than 1.5 times the interquartile range away from the bottom or top of the box.

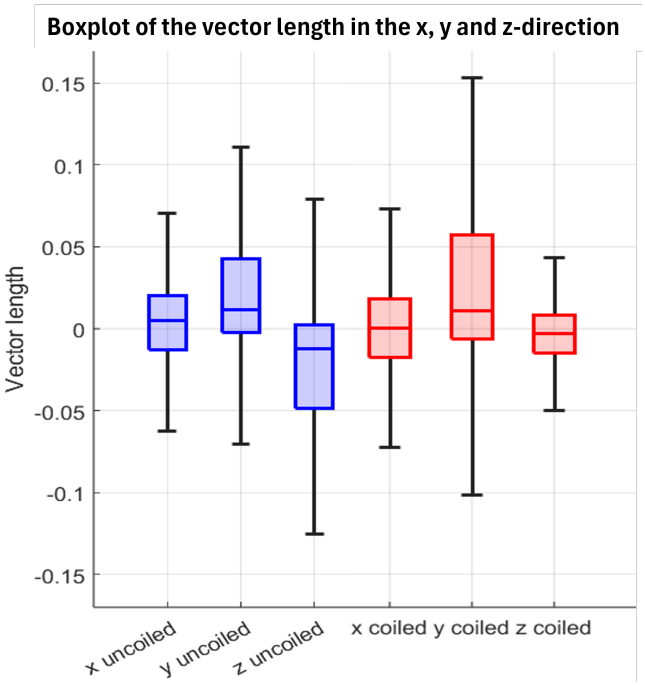

Figure 3.10: The box plot of the uncoiled (blue) and coiled (red) length of flow velocity vectors in the x, y and z direction.

In the case of stationary fluid, the vector lengths would be normally distributed. Therefore, the median would lay in the middle of the box and both whiskers would be equal in size. The box plot of both x flows are close to normally distributed, this also accounts for the z coiled measurement. Between the coiled and uncoiled y-flow a clear difference in distribution is shown. The medians are close together, but the interquartile range of the coiled flow is almost one and a half times as big. This shows that the lengths in the coiled y-flow are more spread out than the uncoiled measurement, but both lie around the same median.

3.4.2 Curl analysis

The magnitudes of the curl vectors are averaged for each pixel in the y-direction. The blue line displays the uncoiled curl magnitude and the red line the coiled. In gray, the AVM is displayed to indicate the location of the curl. The location of the coil is also displayed in red. It is seen that throughout the whole AVM the curl is higher in the coiled AVM, this shows a higher circulation. The largest differences in curl are seen in the target location of the coil. However, in the aneurysmal part of the AVM the curl is also noticeably higher in the coiled AVM than the uncoiled AVM.

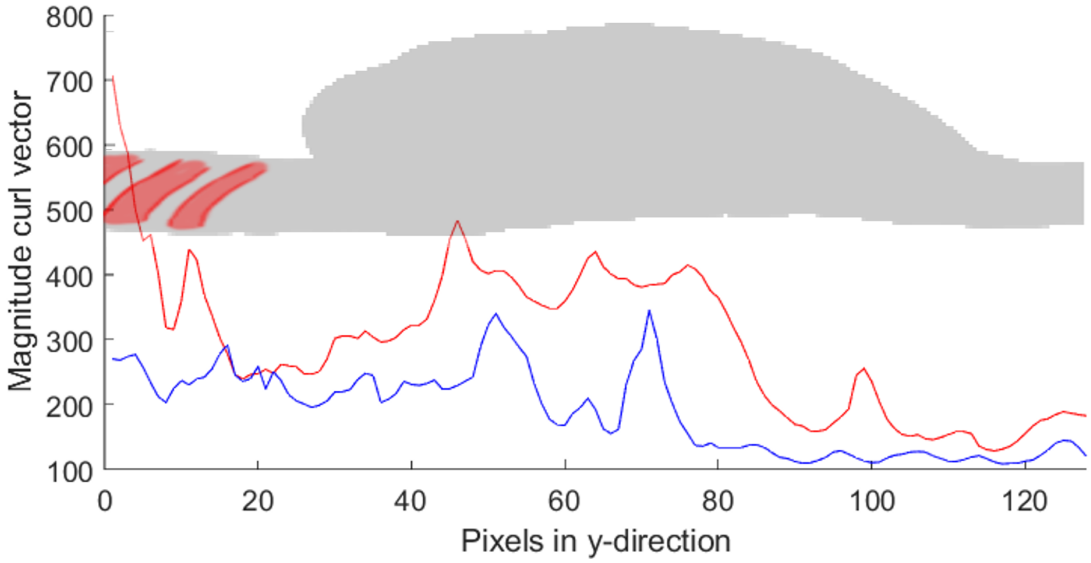

Figure 3.11: The magnitude of the crul vector displayed as an average for each pixel in the y direction. In combination with the AVM displayed in gray and the coil drawn in red.

3.4.3 Flow profile

To analyse the effect of the coil, the flow profile is visualized as a cross-section. This cross-section is taken just before entering the AVM which is also shown bottom right corner of figure 3.12. The uncoiled AVM shows a smooth transition of the lower velocities on the side of the vessel and the higher velocities in the middle. However, the highest velocity is located more towards the right wall than the middle of the vessel. The coiled AVM shows a rougher surface with the highest and lowest velocity next to each other. This looks slightly like aliasing, but that is not possible because the configured VENC velocity of 0.5 m/s was not reached, as can be seen in the side profile of the flow velocity profile when plotted in 3D. The cross-section also shows that the form of the feeding artery different, the uncoiled is a more oval shape instead of a circle.

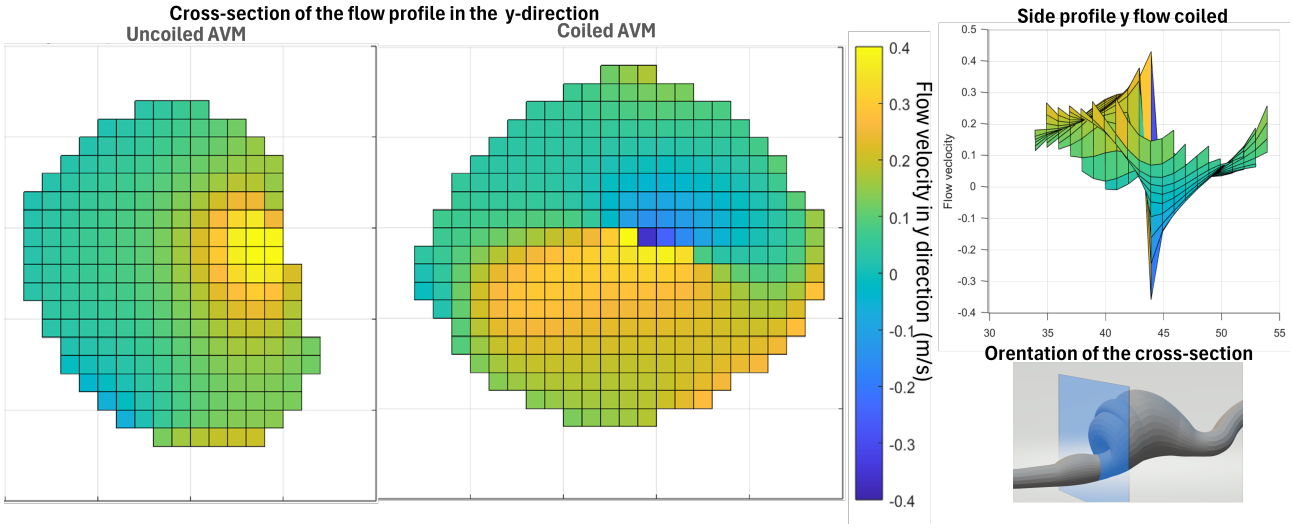

Figure 3.12: The flow profile of the uncoiled a coiled AVM the orientation of the slice is seen in the bottom right corner. The side profile of the flow profile is seen in the top right corner.

Chapter 4

Discussion

This discussion compares the flow patterns of an uncoiled and coiled AVM, measured with 4D flow MRI. For this measure to be taken, a coil needed to be modelled and placed in the AVM. The production method of the plastic coil was a self-developed method and worked very well, and the produced coils were great for this experiment. The choice in diameter for the wire of the coil was limited, and therefore not an exact scaled version of a clinical embolization. However, this does not have significant imitations to this research because validation data is made for a CFD and in a CFD model the coil dimensions can be adjusted.
The implementation of the technique was the best possible with the materials in reach. The principles of a clinical implementation were taken en modelled to be used in this model. In addition, it would be very interesting to experiment with longer coils and different and more complex AVMS.

The results so that the implantation of a small plastic coil just before the AVM has large influences on the flow though the AVM. This can be seen in the comparison of the absolute flow slices in figure 3.8 and in the absolute flow and coil image in figure 3.9. The quantification of these flow patterns shows that the flow though the AVM (the y-direction) is disrupted. The spread in the y direction is almost one and a half times as big, while the average flow is close to equal. The embolization of the AVM also lead to more circulation, which indicates a chaotic flow. The coil gives rise to a higher circulation and this works throughout the AVM. The flow profile lead to a comparable flow result as a thrombus in a vessel mentioned by K. Freson in her simulation of a thrombus in a 3D model. The positive flow on one side and the negative flow on the other, as is also seen in figure 3.12 [21].

The goal of a coiled embolization treatment is to occlude the feeding branches of the AVM, so the flow though the AVM diminishes [22]. However, this was not the goal of the embolization procedure done in this research. Occluding the feeding artery was not possible because there is no capillary network in this model, so the fluid has to move through the AVM. The effects of a complete embolization could not be analysed, only a change in the flow patterns by placing a small coil are analysed. Therefore, a recommendation for further research would be to use a simplified capillary network surrounding the AVM. So a higher resistance of a coiled AVM would result in more blood flow through the capillaries. This also adds the possibility to apply embolizations until the AVM is completely blocked.

The z-flow vector fields show large differences that were not expected. A possible explanation could be the different orientation of the AVMs. This could also be an explanation of the oval formed cross-section in figure 3.12. Between each measurement the AVM must be taken out to check for air bubbles, and in case of embolization the AVM must be changed to the coiled version. For the analyses of the data, a solid cylinder with a hollow AVM inside would result in more consistent results that would be easier to compare. This could also show absolute results in the flow as an effect of the coil, by subtraction the matrices from each other.

In this research, multiple attempt were done to measure the minimum and maximum velocity through the AVM, taken from the pulsatile flow in figure 2.2. The minimum measurement resulted in a decent result, but the maximum measurement was too bad to publish. Therefore, the decision was made not to use both of these measurements. However, the combination of these measurements would provide interesting information and more possibilities to analyse and compare the effects of coiled embolization.

Chapter 5

Conclusion

In conclusion, a coiled embolization was performed using an AVM phantom with a hand-made coil and catheter, which resulted in a possibility to measure the flow effect of a coil in an AVM with 4D flow MRI. The most relevant effect being the disrupted flow straight through the AVM measured in a higher spread of vector lengths in the flow direction. In combination with the heightened curl in the coil itself, but also in the aneurysmal zone of the AVM. This circulation is also shown in the flow profile. For further applications, 4D flow MRI can be used to generate more data to validate CFD models. This could be done in many ways, I would recommend using a (simplified) capillary network surrounding the AVM. So a higher resistance of a coiled AVM would result in more blood flow through the capillaries. In combination with stationary AVM, so no rotation is possible between measurements. This research was a small step towards creating a complete AVM CFD models that could inform and optimise embolisation intervention.

References

[1] Yakes W, Baumgartner I. Interventional Treatment of Arterio-Venous Malformations. Gefasschirurgie. 2014;19(4):325-30.

[2] Zyck S, Davidson CL, Sampath R. Arteriovenous Malformations of the Central Nervous System. In: StatPearls [Internet]. StatPearls Publishing; 2024. Available from: https://www.ncbi.nlm.nih.gov/books/NBK531479.

[3] Uller W, Alomari AI, et al. Arteriovenous Malformations. Seminars in Pediatric Surgery. 2014;23(4):203-7.

[4] Neurochirurgisch Centrum Zwolle. Arterio veneuze malformatie - Neurochirurgisch Centrum Zwolle; 2016. Available from: https://neurochirurgie-zwolle.nl/patienteninformatie/schedel-en-hersenen/arterio-veneuze-malformatie.

[5] Ansari SA, Schnell S, Carroll T, Vakil P, Hurley MC, Wu C, et al. Intracranial 4D Flow MRI: Toward Individualized Assessment of Arteriovenous Malformation Hemodynamics and Treatment-Induced Changes. AJNR Am J Neuroradiol. 2013 Oct;34(10):1922.

[6] Gaia Franzetti, and Mirko Bonfanti, and Tanade, Cyrus. A Computational Framework for Pre-Interventional Planning of Peripheral Arteriovenous Malformations. Cardiovasc Eng Technol. 2022 Apr;13(2):234-46.

[7] Velocity encoding (VENC); 2024. [Online; accessed 8. Jul. 2024]. Available from: https://mriquestions.com/what-is-venc.html.

[8] Phase Contrast MRA; 2024. [Online; accessed 8. Jul. 2024]. Available from: https://mriquestions.com/phase-contrast-mra.html.

[9] Bougardt J. IN-VITRO AND IN-SILICO MODELLING OF ARTERIOVENOUS MALFORMATIONS FOR SURGICAL PLANNING.

[10] Mostafa E, Graefe SB, Varacallo M. Anatomy, Bony Pelvis and Lower Limb: Leg Posterior Compartment. In: StatPearls [Internet]. StatPearls Publishing; 2023. Available from: https://www.ncbi.nlm.nih.gov/books/NBK537340.

[11] Marieb EN. Essentials of Human Anatomy & Physiology. Redwood City, Calif.: Benjamin/Cummings Publishing Company; 1991.

[12] Bodnár T, Sequeira A, Prosi M. On the shear-thinning and viscoelastic effects of blood flow under various flow rates. Applied Mathematics and Computation. 2011;217(11):5055-67.

[13] Perrira N, Shuib AS, Phang SW, Muda AS. Experimental Investigation of Blood Mimicking Fluid Viscosity for Application in 3D-Printed Medical Simulator. J Phys Conf Ser. 2022 May;2222(1):012016.

[14] Cook Medical Coils | How it works; 2024. [Online; accessed 8. Jul. 2024]. Available from: https://www.cookmedical.com/interventional-radiology/coils-home/how-it-works.

[15] MReye® Embolization Coil | Cook Medical; 2024. [Online; accessed 8. Jul. 2024]. Available from: https://www.cookmedical.com/products/di_mreye_webds.

[16] Trerotola SO, Pressler GA, Premanandan C. Nylon Fibered Versus Non-Fibered Embolization Coils: Comparison in a Swine Model. J Vasc Interv Radiol. 2019 Jun;30(6):949-55.

[17] Xometry T. 7 Properties of Nylon: Everything you Need to Know. Xometry. 2024 May. Available from: https://www.xometry.com/resources/materials/properties-of-nylon.

[18] Xometry T. Nylon: Uses, Types, and Materials. Xometry. 2022 Jun. Available from: https://www.xometry.com/resources/materials/nylon.

[19] Mean vs Median - Difference and Comparison | Diffen; 2023. [Online; accessed 8. Jul. 2024]. Available from: https://www.diffen.com/difference/Mean_vs_Median.

[20] Thomas GB, Weir MD, Hass J. Thomas' Calculus. 14th ed. Boston: Pearson; 2018.

[21] Wang W, Diacovo TG, Chen J, Freund JB, King MR. Simulation of Platelet, Thrombus and Erythrocyte Hydrodynamic Interactions in a 3D Arteriole with In Vivo Comparison. PLoS One. 2013;8(10).

[22] Wei Zhou MD, Peter H Lin MD, Andres Eraso MD, Alan B Lumsden MD. Embolotherapy of Peripheral Arteriovenous Malformations. Endovascular Today. 2005 Nov. Available from: https://evtoday.com/articles/2005-nov/EVT1105_F7_Lumsden.html.

Appendix A

Blood Mimicking Fluid (BMF) Information and preperation

Written by Jordan Bougardt

A.1 Background Information

As you know, whole blood is a fluid made up of several components categorised into the liquid fraction and cellular fractions. For the purposes of my study only the liquid fraction is being modelled and so to maintain accuracy in the modelling procedure, the shear-thinning nature of whole blood had to be replicated experimentally. This is where this so-called "Blood Mimicking Fluid" comes into play. Figure A.1 is a comparison between the viscosity-shear rate curve of the final BMF mixture and that of true blood. The final BMF mixture composition was determined through rheological testing which I have explained further in the following section.

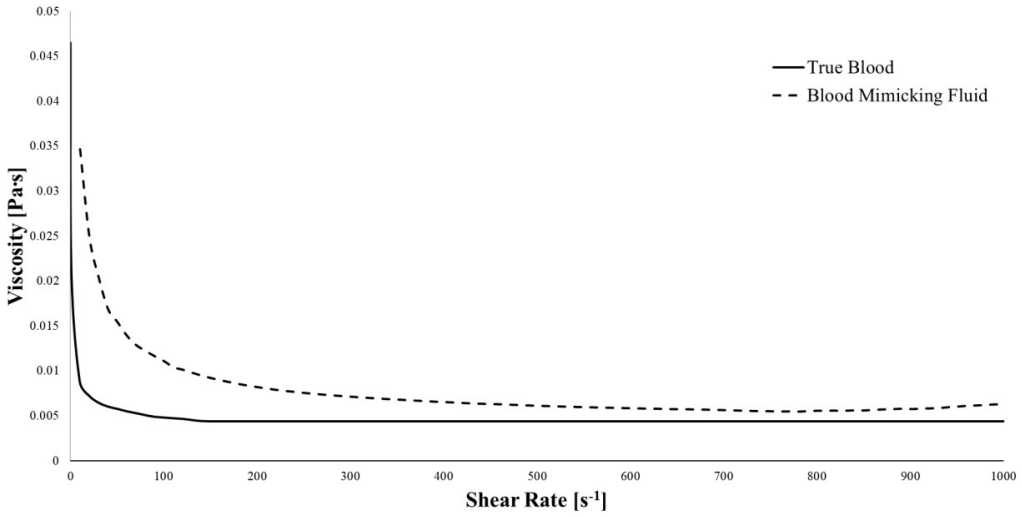

Figure A.1: Figure 1: True Blood versus Blood Mimicking Fluid Non-Newtonian comparison.

A.2 BMF Preparation Guide

Through rheological experimentation, it was found that by mixing distilled water, glycerol, and xanthan gum in the ratio detailed in Table A.1, a suitable replication of blood's non-Newtonian, shear-thinning nature could be achieved.
Lastly, I have prepared a list of steps that you can follow to make sure that you achieve a homogenous solution when creating the BMF mixture. The BMF Water-Glycerol-Xantham gum mixture should be prepared as follows to ensure that you achieve a homogenous solution:

Table A.1: Table 1: Composition of the Blood Mimicking Fluid by weight percentage.

Distilled water [wt%]	Glycerol [wt%]	Xanthan Gum [wt%]
95	4.93	0.07

1. 1) Glycerol will be introduced into a standard beaker and prepared by mixing at a rate of 300 rpm for 2 minutes.
2. 2) Xantham gum is weighed and gradually added into the vortex of the mixing glycerol to ensure adequate mixing and to prevent lump formation.
3. 3) The mixture is mixed for 15 minutes at a rate of 400 rpm.
4. 4)Water is gradually added into the vortex of the mixture and the mixture is left to mix for an additional 15 minutes at a rate of 600 rpm.

You may not have a mixer that is capable of direct speed control, which is fine. Just try to keep up with the mixing times and the increasing rates of rotation required. Make sure that there are no visible clumps of Xanthan gum before starting step 4 and try to prepare the mixture in an environment with a temperature that is stable and above 20°C.
If you follow these steps I am sure that you will be able to achieve a homogenous solution fairly easily!